Supplementary Methods

Fitting procedure and computation of QD surface density from UV-visible spectroscopy
As quantum systems made of discret states, CdTe QDs are described by the following optical susceptibility [1]:

$$\chi^{(1)}_{\mathrm{QD}}(\omega) = \sum_n \frac{N|p_n|^2}{\hbar\varepsilon_0}\left(\frac{-1}{\omega-\omega_n+\imath\gamma_n}+\frac{1}{\omega+\omega_n+\imath\gamma_n}\right). \tag{1}$$

In this equation, obtained within the effective mass approximation, N is the QD density and n itemizes the excitonic states: for the n^{th} exciton, p_n is the dipole moment, γ_n the damping constant, and ω_n the eigenenergy whose expression is [1, 2, 3]:

$$\hbar\omega_n = E_0 + \frac{\hbar^2\alpha_n^2}{2m_{\mathrm{e}}R^2} + \frac{\hbar^2\beta_n^2}{2m_{\mathrm{h}}R^2} - \frac{c_n e^2}{4\pi\varepsilon_0\epsilon R}. \tag{2}$$

R represents the radius of NCs, here considered as spheres, and $\epsilon = 10.2$ the dielectric constant of bulk CdTe. The constant E_0 includes the band gap energy of bulk CdTe (1.61 eV at 4 K), the exciton Rydberg energy ($\sim$ 10 meV), and may also take into account the self-polarization energy of NCs depending on the polarizability of their surroundings [3]. Moreover, the second and third terms correspond to the confinement energies of the electron and the hole, while the fourth one is their attractive Coulomb interaction. For any excitonic state, the effective mass of the electron is $m_{\mathrm{e}} = 0.096m_0$, where m_0 is the electron bare mass [4]. For the hole, $m_{\mathrm{h}} = 0.11m_0$ (light hole) or $m_{\mathrm{h}} = 0.69m_0$ (heavy hole) according to the type of exciton [4]. For the sake of clarity, **Supplementary Table 1** gives the nature of the hole and the coefficients α_n, β_n and c_n for the three excitonic states considered in this article. The next subsection of Supplementary Methods shows how c_n is computed.

Amongst all these physical quantities, p_n, γ_n and E_0 are unknown and must be determined experimentally. Since UV-visible absorption depends on the imaginary part of $\chi^{(1)}_{\mathrm{QD}}$ [1], we can extract these parameters by fitting the absorbance spectrum of a colloidal CdTe QDs solution. Assuming further a gaussian size distribution, the absorbance $\mathcal{A}(\omega)$ of such a solution reads:

$$\mathcal{A}(\omega) = \int_0^{+\infty} \mathrm{d}R\ \mathcal{A}_R(\omega)\ \frac{\exp\left(-\frac{(R-R_0)^2}{2\sigma^2}\right)}{\sigma\sqrt{2\pi}}, \tag{3}$$

with [1]:

$$\mathcal{A}_R(\omega) = \frac{\ell}{c\ln 10}\ \frac{\omega}{\sqrt{\epsilon}}\ \mathrm{Im}\chi^{(1)}_{\mathrm{QD}}(\omega). \tag{4}$$

The resulting fitting parameters are given in **Supplementary Table 2**.

For the CaF_2 prism grafted with CdTe NCs, the surface density N_s (which plays the role of $N \times \ell$ in equations (1) and (4)) and the size dispersion σ are henceforth the only two fitting parameters. Given $N_s = 6.6\ 10^{18}$ m^{-2} (deduced from fitting) and $R_0 = 1.7$ nm [5], an estimation of the layer thickness is $t \sim 2R_0 \times \frac{N_s}{(2R_0)^{-2}} = (2R_0)^3 N_s$. Indeed, $2R_0$ and $(2R_0)^{-2}$ roughly correspond to the thickness and surface density of a QD monolayer, and then $N_s/(2R_0)^{-2}$ to the number of monolayers.

Exciton energies and computation of the coefficients c_n
The eigenenergy of the n^{th} excitonic state is given by:

$$\hbar\omega_n = E_0 + \frac{\hbar^2\alpha_n^2}{2m_{\mathrm{e}}R^2} + \frac{\hbar^2\beta_n^2}{2m_{\mathrm{h}}R^2} - \frac{c_n e^2}{4\pi\varepsilon_0\epsilon R}.$$

Let us call $\psi_{\mathrm{e},n}$ and $\psi_{\mathrm{h},n}$ the associated electron and hole wave functions. The coefficient c_n is defined as:

$$\frac{c_n}{R} = \int_{\mathbb{R}^3}\mathrm{d}\mathbf{r}_{\mathrm{e}}\int_{\mathbb{R}^3}\mathrm{d}\mathbf{r}_{\mathrm{h}}\ |\psi_{\mathrm{e},n}(\mathbf{r}_{\mathrm{e}})|^2\frac{1}{|\mathbf{r}_{\mathrm{e}}-\mathbf{r}_{\mathrm{h}}|}|\psi_{\mathrm{h},n}(\mathbf{r}_{\mathrm{h}})|^2, \tag{5}$$

where $\mathbf{r}_{\mathrm{e}}$ and $\mathbf{r}_{\mathrm{h}}$ describe the respective positions of the electron and the hole, and R is the radius of the nanocrystal. According to ref. [1] and [6], the generic form of the wave functions is:

$$\psi(r,\theta,\phi) = \sqrt{\frac{2}{R^3}}\ \frac{j_\nu(x_{\nu l}\ r/R)}{j_{\nu+1}(x_{\nu l})}\ \mathcal{Y}_{lm}(\theta,\phi), \tag{6}$$

where $z \to j_\nu(z)$ is the spherical Bessel function of order ν, and $x_{\nu l}$ its l^{th} zero. The functions $\mathcal{Y}_{lm}$ refer to the spherical harmonics. In the article, we take into account the first three excitonic states, itemized by

$1 \leqslant n \leqslant 3$, whose characteristics are given in **Supplementary Table 3**. We then compute numerically (in C language with Xcode) the coefficients c_1, c_2 and c_3 by combining equations (5) and (6). For the first excitonic state, we find the same value than that computed by Y. Kayanuma [7]: $c_1 = 1.78$.

Computation of Fresnel factors within SFG spectroscopy three-layer model

In order to compute the SFG Fresnel factors $L_{ijk}(\omega_{\rm vis}, \omega_{\rm IR})$ for our sample, we use the three-layer model as schemed in **Supplementary Figure 1**. These factors play an important role in $\chi^{(2)}_{\rm ppp}$:

$$\begin{aligned}\chi^{(2)}_{\rm ppp} \;=\; & -L_{xxz}\ \cos\theta^{\rm R}_{\rm SFG}\ \cos\theta^{\rm R}_{\rm vis}\ \sin\theta^{\rm R}_{\rm IR}\ \chi^{(2)}_{xxz} \\ & -L_{xzx}\ \cos\theta^{\rm R}_{\rm SFG}\ \sin\theta^{\rm R}_{\rm vis}\ \cos\theta^{\rm R}_{\rm IR}\ \chi^{(2)}_{xzx} \\ & +L_{zxx}\ \sin\theta^{\rm R}_{\rm SFG}\ \cos\theta^{\rm R}_{\rm vis}\ \cos\theta^{\rm R}_{\rm IR}\ \chi^{(2)}_{zxx} \\ & +L_{zzz}\ \sin\theta^{\rm R}_{\rm SFG}\ \sin\theta^{\rm R}_{\rm vis}\ \sin\theta^{\rm R}_{\rm IR}\ \chi^{(2)}_{zzz}.\end{aligned}$$

Within the three-layer model, the coefficients L_{ijk} are given by:

$$L_{ijk}(\omega_{\rm vis}, \omega_{\rm IR}) \;=\; F_{ii}(\omega_{\rm vis} + \omega_{\rm IR})\ F_{jj}(\omega_{\rm vis})\ F_{kk}(\omega_{\rm IR}), \tag{7}$$

where:

$$F_{xx}(\omega_u) \;=\; \frac{2\ n_1(\omega_u)\cos\theta^{\rm T}_u}{n_1(\omega_u)\cos\theta^{\rm T}_u + n_2(\omega_u)\cos\theta^{\rm R}_u}, \tag{8}$$

$$F_{yy}(\omega_u) \;=\; \frac{2\ n_1(\omega_u)\cos\theta^{\rm R}_u}{n_1(\omega_u)\cos\theta^{\rm R}_u + n_2(\omega_u)\cos\theta^{\rm T}_u}, \tag{9}$$

and:

$$F_{zz}(\omega_u) \;=\; \frac{2\ n_2(\omega_u)\cos\theta^{\rm R}_u}{n_1(\omega_u)\cos\theta^{\rm T}_u + n_2(\omega_u)\cos\theta^{\rm R}_u}\ \left(\frac{n_1(\omega_u)}{n_{\rm lay}(\omega_u)}\right)^2. \tag{10}$$

The subscript u refers to 'vis', 'IR' or 'SFG'. In our configuration:

$$\theta^{\rm R}_{\rm vis} = 55^\circ, \qquad \theta^{\rm R}_{\rm IR} = 65^\circ, \qquad \theta^{\rm R}_{\rm SFG} = \arcsin\left(\frac{\omega_{\rm vis}\sin\theta^{\rm R}_{\rm vis} + \omega_{\rm IR}\sin\theta^{\rm R}_{\rm IR}}{\omega_{\rm vis} + \omega_{\rm IR}}\right), \tag{11}$$

and:

$$\theta^{\rm T}_u = \arcsin\left(\frac{n_1(\omega_u)\sin\theta^{\rm R}_u}{n_2(\omega_u)}\right). \tag{12}$$

Thus, we computed the four SFG Fresnel factors displayed in Figure 2c by combining these equations. For the refractive index $n_1(\omega)$ of CaF_2, we relied on the ref. [8], while the refractive index $n_2(\omega)$ of air was considered equal to 1. Besides, the refractive index $n_{\rm lay}(\omega)$ of the QD layer is determined in the article.

Processing of the SFG spectra

The measurement of the SFG intensity $I_{\rm SFG}$ gives access to the effective second-order susceptibility $\chi^{(2)}_{\rm ppp}$ according to ref. [9]:

$$I_{\rm SFG} = \frac{8\pi^3\omega^2_{\rm SFG}}{c^3\cos^2\theta^{\rm R}_{\rm SFG}}\left|\chi^{(2)}_{\rm ppp}\right|^2 I_{\rm vis} I_{\rm IR}. \tag{13}$$

The SFG frequency $\omega_{\rm SFG}$, the angle $\theta^{\rm R}_{\rm SFG}$, and the input intensities $I_{\rm vis}$ and $I_{\rm IR}$ are known. Then, we can extract $\left|\chi^{(2)}_{\rm ppp}\right|^2$ (in arbitrary units, since we get rid of the constant factors):

$$\left|\chi^{(2)}_{\rm ppp}\right|^2 = \frac{\cos^2\theta_{\rm SFG}}{\omega^2_{\rm SFG}K(\omega_{\rm SFG})}\ \frac{I_{\rm SFG}}{I_{\rm vis}I_{\rm IR}}. \tag{14}$$

Here, $K(\omega_{\rm SFG}) = K^2_{\rm grat.}(\omega_{\rm SFG}) \times K_{\rm PM}(\omega_{\rm SFG})$, where $K_{\rm grat.}$ and $K_{\rm PM}$ are the respective efficiencies of the gratings and the photomultiplier which compose the monochromator we use to measure $I_{\rm SFG}$. The SFG spectra presented in Figure 4a are normalized following this procedure.

The SFG spectra of the article are fitted with five molecular vibration modes:

$$\chi^{(2)}_{\rm ppp} = A\ e^{\imath\Phi} + \sum_{v=1}^{5}\frac{a_v\ e^{\imath\varphi_v}}{\omega_v - \omega_{\rm IR} + \imath\gamma_v}. \tag{15}$$

The fitting parameters associated to the fitting curves presented in Figure 4 are given in **Supplementary Table 4**.

In Figure 4c, we draw the mean amplitudes $\bar{a}(\lambda_{\text{vis}}) = \frac{1}{5}\sum_{v=1}^{5} a_v(\lambda_{\text{vis}})$. For each visible wavelength λ_{vis}, the relative uncertainty $\frac{\Delta\bar{a}}{\bar{a}}$ is estimated according to:

$$\frac{\Delta\bar{a}(\lambda_{\text{vis}})}{\bar{a}(\lambda_{\text{vis}})} = \text{rsd}\left\{\frac{a_v(\lambda_{\text{vis}})}{\langle a_v\rangle}\right\}_{1\leqslant v\leqslant 5}, \tag{16}$$

where $\langle a_v\rangle = \frac{1}{5}\sum_{\lambda_{\text{vis}}} a_v(\lambda_{\text{vis}})$, and 'rsd' refers to the relative standard deviation. Indeed, for a given visible wavelength λ_{vis}, the amplitudes $a_v(\lambda_{\text{vis}})$, $1 \leqslant v \leqslant 5$, are weighted by $1/\langle a_v\rangle$ to be comparable to each other. For the sake of clarity, **Supplementary Figure 2** illustrates equation (16).

Exciton	Electron-hole states	α_n	β_n	c_n
$n=1$	$1S_e$, $1S_{hh}$	3.14	3.14	1.78
$n=2$	$1S_e$, $1D_{hh}$	3.14	5.76	1.52
$n=3$	$1S_e$, $1S_{lh}$	3.14	3.14	1.78

Supplementary Table 1 – **First excitonic states of CdTe NCs.** Characteristics of the three excitonic states used for fitting UV-visible spectra. The second column gives the electron-hole configuration of each exciton following the convention of ref. [1]. Especially, 'hh' refers to heavy holes and 'lh' to light holes. The parameters α_n and β_n are extracted from ref. [1]. The calculation of the parameters c_n is detailed in Supplementary Methods.

Parameter	Fitting value
E_0	0.93 eV
σ	4%
p_1	12.7 D
γ_1	0.0018 eV
p_2	16.4 D
γ_2	0.088 eV
p_3	13.0 D
γ_3	0.0022 eV

Supplementary Table 2 – **Fit to the UV-visible spectrum of reference colloidal solution.** Results of the fitting procedure based on equations (1) to (4) and applied to the experimental UV-visible spectrum of Figure 2a. The corresponding curve is displayed in the same graph.

Exciton	Electron/hole states	(ν, l)	$x_{\nu l}$	c_n
$n=1$	$1S_e$	$(1,0)$	3.14 (α_1)	1.78
	$1S_{hh}$	$(1,0)$	3.14 (β_1)	
$n=2$	$1S_e$	$(1,0)$	3.14 (α_2)	1.52
	$1D_{hh}$	$(1,2)$	5.76 (β_2)	
$n=3$	$1S_e$	$(1,0)$	3.14 (α_3)	1.78
	$1S_{lh}$	$(1,0)$	3.14 (β_3)	

Supplementary Table 3 – **Exciton quantum numbers.** Characteristics of the three excitonic states considered in the article.

λ_{vis} (nm)	**450**	**488**	**520**	**568**	**612**
A	2.53	3.25	2.02	2.79	2.32
Φ			3.14		
a_1	38.7	70.6	57.2	36.5	25.2
ω_1			2862 cm^{-1}		
γ_1			12 cm^{-1}		
a_2	23.2	56.6	46.8	36.0	23.0
ω_2			2884 cm^{-1}		
γ_2			8 cm^{-1}		
a_3	104.1	134.9	106.9	84.2	28.4
ω_3			2912 cm^{-1}		
γ_3			10 cm^{-1}		
a_4	53.0	61.4	60.5	45.0	32.4
ω_4			2935 cm^{-1}		
γ_4			7 cm^{-1}		
a_5	26.0	31.5	29.1	23.5	21.3
ω_5			2967 cm^{-1}		
γ_5			6 cm^{-1}		

Supplementary Table 4 – **Fit to the SFG spectra of CaF_2/QD/air interface.** Fitting parameters extracted from the SFG spectra displayed in Figure 4 according to equation (15), *i.e* equation (3) in the article. All the phases φ_v are set to zero.

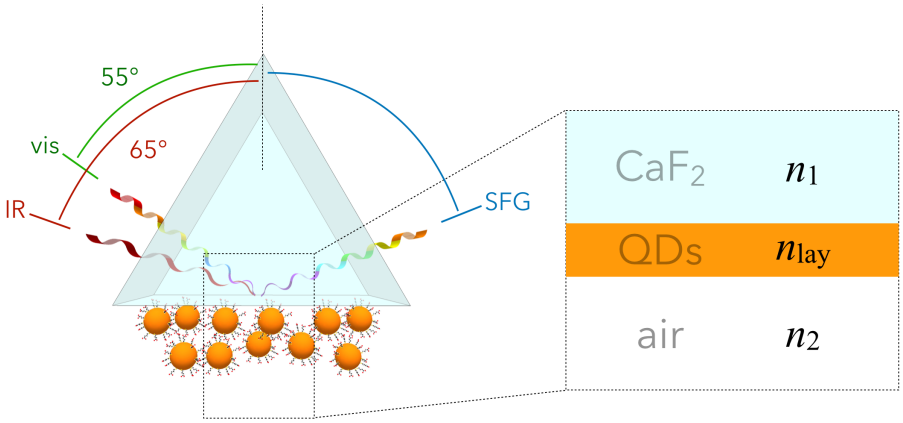

Supplementary Figure 1 – Three-layer model. Sketch of the CaF_2/QD/air interface within the three-layer model. n_1, n_{lay} and n_2 are the refractive indexes associated respectively to the three materials.

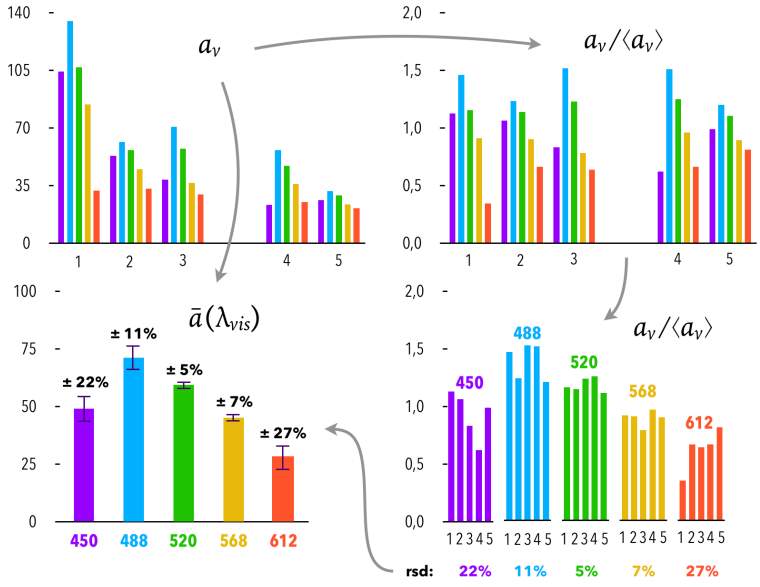

Supplementary Figure 2 – Computation of relative standard deviations for vibration amplitudes. Illustration of equation (16) showing how the relative standard deviations of the mean amplitudes $\bar{a}(\lambda_{\text{vis}})$ are determined for each visible wavelength λ_{vis}.

Supplementary Note 1 – Structural properties of $CdTe_xS_{1-x}$ QDs. XPS measurements evidence that the commercial QDs we use are ternary alloys $CdTe_xS_{1-x}$ with $x = 0.25$. This result is quite surprising given the characteristics provided by the manufacturer, but in real accordance with the UV-visible characterization. According to ref. [3, 10, 11, 12, 13], we would expect a first local maximum of absorption around 570 nm. Figures 2a and 4b clearly show that it is not the case: this maximum is reached for a wavelength of $\lambda_{\max} = 488$ nm. From theory, the position of this maximum is related to the QD band gap E_g:

$$\lambda_{\max} = \frac{hc}{E_g}, \tag{17}$$

where h is the Planck constant and c the velocity of light in vacuum. In virtue of Vegard's law [14, 15], the gap of a ternary alloy $CdTe_xS_{1-x}$ can be approximated by:

$$E_g(CdTe_xS_{1-x}) = x\ E_g(CdTe) + (1-x)\ E_g(CdS). \tag{18}$$

Rigorously, this law can be used if it is first satisfied by the lattice parameters a:

$$a(CdTe_xS_{1-x}) = x\ a(CdTe) + (1-x)\ a(CdS). \tag{19}$$

In our case, with $x = 0.25$, the lattice parameter of QDs is expected to be:

$$a(\text{QDs}) = 0.25\ a(CdTe) + 0.75\ a(CdS). \tag{20}$$

Given that $a(CdTe) = 6.48$ Å and $a(CdS) = 5.82$ Å [10], we get $a(\text{QDs}) = 5.98$ Å. From ref. [5], the structural characterization of these commercial QDs with High-Resolution Transmission Electron Microscopy leads to $a(\text{QDs}) = 5.86$ Å. We deduce that the deviation from Vegard's law is up to -2%.

Thanks to the same study [5], we know that the QDs we use have a mean diameter $d_0 = 3.4$ nm. From ref. [10], we obtain in this case $E_g(CdTe) = 2.18$ eV and $E_g(CdS) = 2.76$ eV. Then, equation (18) gives $E_g(CdTe_{0.25}S_{0.75}) = 2.62$ eV. Applying a deviation of -2%, we eventually get $E_g(\text{QDs}) = 2.57$ eV, which corresponds to a wavelength of 481 nm, close to the expected 488 nm. To conclude, the substitution of tellurium by sulfur in the core of QDs is in accordance with the UV-visible measurements.

Supplementary Note 2 – Description of vibration modes. Given a molecule of N atoms labeled by $p \in [\![1, N]\!]$, let us call (x_p, y_p, z_p) the displacement vector of atom p from its equilibrium in cartesian coordinates. In virtue of the formalism of ref. [16], we define the mass-weighted cartesian coordinates $\{q_n\}_{n=1}^{3N}$ by:

$$\begin{array}{llll} (\bar{n}=1) & q_1 = \sqrt{m_1}x_1 & q_4 = \sqrt{m_2}x_2 & \\ (\bar{n}=2) & q_2 = \sqrt{m_1}y_1 & q_5 = \sqrt{m_2}y_2 & \cdots \\ (\bar{n}=0) & q_3 = \sqrt{m_1}z_1 & q_6 = \sqrt{m_2}z_2 & \end{array} \tag{21}$$

We notice that all the coordinates q_n for which n is congruent to 1 modulo 3 (*i.e.* $\bar{n} = 1$ with the present notations) are related to the x-coordinates of the associated atoms. When n is congruent to 2 modulo 3 (*i.e.* $\bar{n} = 2$), q_n is related to the y-coordinate, and if n is congruent to 0 modulo 3 (*i.e.* $\bar{n} = 0$), q_n is related to the z-coordinate. This explain the sum partition of equation (31).

The potential energy V of a molecule described by $\{q_n\}_{n=1}^{3N}$ naturally depends on all these coordinates and can be expanded as follows [16]:

$$V = \frac{1}{2}\sum_{n,m}\left(\frac{\partial^2 V}{\partial q_n \partial q_m}\right)_0 q_n q_m. \tag{22}$$

Matrix $\boldsymbol{f} = (f_{nm})$ is then defined as:

$$f_{nm} = \left(\frac{\partial^2 V}{\partial q_n \partial q_m}\right)_0, \quad \text{so that} \quad V = \frac{1}{2} f_{nm} q^n q^m. \tag{23}$$

Supplementary Note 3 – Analytical calculation of molecular SFG response. We developed an unusual and original method based on dielectrics, nonlinear optics and Fourier analysis. First, we describe the vibration modes of ligands as normal modes. In the formalism of ref. [16], the normal coordinates $\{Q_v\}_{v=1}^{3N}$ are linear combinations of the mass-weighted cartesian coordinates $\{q_n\}_{n=1}^{3N}$, where N is the number of atoms which compose the molecule. It exists a matrix $\boldsymbol{l} = (l_{nv})$ so that:

$$Q_v = \sum_n l_{nv} q_n. \tag{24}$$

The coordinates $q_n(t)$ satisfy the following equations of motion [16]:

$$\ddot{q}_n(t) + f_{nm}\ q^m(t) = 0. \tag{25}$$

For simplicity, we use the Einstein convention to write all the sums: $A_iB^i = A^iB_i = \sum_i A_iB_i$. The general solutions read $q_n(t) = q^v_{n,0}\cos(\omega_v t)$, where ω_v^2 is one of the eigenvalues of matrix $\boldsymbol{f} = (f_{nm})$, *i.e.* $f_{nm}q^m = \omega_v^2 q_n$, and $q^v_{n,0}$ a constant depending on the initial conditions. The eigenvalue ω_v corresponds to the frequency of the normal mode v. In presence of an external electric field $\mathbf{E}$, equation (25) reads:

$$\ddot{q}_n(t) + f_{nm}\ q^m(t) = e_n E_{\bar{n}}(t), \tag{26}$$

where e_n is a constant depending on the electronic charge and the mass of the associated atom. The subscript $\bar{n}$ refers to the congruence classes of the integers n for a modulus 3. Here, $\bar{n} = 0$, 1 or 2 according to the remainder of the Euclidian division of n by 3. Indeed, for each atom, there are 3 coordinates q_n associated to the three axes x ($\bar{n} = 1$), y ($\bar{n} = 2$) and z ($\bar{n} = 0$) and thus related to $E_x = E_1$, $E_y = E_2$ and $E_z = E_0$, respectively. In frequency Fourier space, equation (26) gives:

$$-\omega^2 q_n(\omega) + \omega_v^2 q_n(\omega) = e_n E_{\bar{n}}(\omega) \implies q_n(\omega) = \frac{e_n E_{\bar{n}}}{\omega_v^2 - \omega^2}. \tag{27}$$

In virtue of the damped harmonic oscillator model, a more reasonable description requires the addition of a damping term $\imath\omega\Gamma_v$:

$$q_n(\omega) = \frac{e_n E_{\bar{n}}}{\omega_v^2 - \omega^2 - \imath\omega\Gamma_v} = e_n D_v(\omega) E_{\bar{n}}, \tag{28}$$

with:

$$D_v(\omega) = \frac{1}{\omega_v^2 - \omega^2 - \imath\omega\Gamma_v}. \tag{29}$$

Equation (24) therefore translates into:

$$Q_v(\omega) = l_{nv}q^n(\omega) = D_v(\omega)\sum_n l_{nv}e_n E_{\bar{n}}(\omega). \tag{30}$$

The three congruence classes constitue a partition of the integers from 1 to $3N$. Hence:

$$\sum_n = \sum_{n|\bar{n}=1} + \sum_{n|\bar{n}=2} + \sum_{n|\bar{n}=0}, \tag{31}$$

i.e.

$$\frac{Q_v(\omega)}{D_v(\omega)} = \underbrace{\sum_{n|\bar{n}=1} l_{nv}e_n}_{=\ g_x}\ E_x + \underbrace{\sum_{n|\bar{n}=2} l_{nv}e_n}_{=\ g_y}\ E_y + \underbrace{\sum_{n|\bar{n}=0} l_{nv}e_n}_{=\ g_z}\ E_z, \tag{32}$$

where we define vector $\mathbf{g} = (g_k)$, so that:

$$Q_v(\omega) = D_v(\omega) g_k E^k(\omega). \tag{33}$$

In the following, we focus on a unique vibration mode and thus omit subscript v.

To account for the NC/ligand coupling, we assume that the ligands feel the local electric field $\mathbf{E}_\ell(\omega) \propto \mathbf{p}(\omega) \propto \boldsymbol{\chi}^{(1)}_{\mathrm{QD}}(\omega)\mathbf{E}(\omega)$ produced by the exciton. In the general case, it exists a tensor $\boldsymbol{\kappa} = (\kappa_{ij})$ so that:

$$\mathbf{E}_\ell = \boldsymbol{\kappa}\mathbf{p}. \tag{34}$$

This tensor depends on the exciton wave function and also contains the spatial dependence of the local electric field (typically, $\kappa_{ij}(r) \sim 1/r^3$). Given the definition of the polarizability tensor $\boldsymbol{\xi} = (\xi_{ij}) \propto \boldsymbol{\chi}^{(1)}_{\mathrm{QD}}$ of a NC, $\mathbf{p}(\omega) = \boldsymbol{\xi}(\omega)\mathbf{E}(\omega)$, where $\mathbf{E}$ is the incident electric field (*i.e.* that of the laser beam). In other words:

$$\mathbf{E}_\ell(\omega) = \underbrace{\boldsymbol{\kappa}\boldsymbol{\xi}(\omega)}_{=\ \tilde{\boldsymbol{\xi}}(\omega)}\mathbf{E}(\omega). \tag{35}$$

This excitonic field is expected to change the molecular dipole moment $\boldsymbol{\mu}$ of the ligands, so that we can write $\boldsymbol{\mu}(\omega) = \boldsymbol{\alpha}(\omega)\mathbf{E}_\ell(\omega) + \boldsymbol{\mu}_0$, where $\boldsymbol{\alpha} = (\alpha_{ij})$ is the polarizability tensor of ligands and $\boldsymbol{\mu}_0$ their dipole moment in the absence of exciton. The molecular dipole moment then reads:

$$\boldsymbol{\mu}(\omega) \ = \ \boldsymbol{\alpha}(\omega)\tilde{\boldsymbol{\xi}}(\omega)\mathbf{E}(\omega) + \boldsymbol{\mu}_0. \tag{36}$$

We know that the efficiency of the IR vibrational response of molecules is driven by the derivative of their dipole moment $\boldsymbol{\mu} = (\mu_i)$ with respect to the normal coordinate Q [16]. To estimate the intensity of the molecular SFG response, we are thus interested in:

$$\frac{\partial \mu_i}{\partial Q} = \underbrace{\frac{\partial \alpha_{ih}}{\partial Q}(\omega)}_{=\ \partial\alpha_{ih}(\omega)}\ \tilde{\xi}^{hj}(\omega)\ E_j(\omega) + \frac{\partial (\mu_0)_i}{\partial Q}. \tag{37}$$

Studying $\frac{\partial (\mu_0)_i}{\partial Q}$ goes back to study the linear IR response of the ligands, as checked in **Supplementary Note 4**. Henceforth, we only consider the first term of equation (37). When they absorb IR light, ligands acquire an oscillating dipole moment with a certain amplitude $\boldsymbol{\Delta\mu}$ which characterizes the strength of the vibrational transition. This transition dipole moment can be expanded according to the normal coordinate, in the vicinity of $Q = 0$:

$$\Delta\mu_i(t) = \left(\frac{\partial \mu_i}{\partial Q}\right)_{Q=0} Q(t). \tag{38}$$

For simplicity, we omit the subscript '$Q = 0$'. In frequency Fourier space, equation (38) is written with a convolution product:

$$\Delta\mu_i(\omega) = \frac{\partial \mu_i}{\partial Q} * Q(\omega). \tag{39}$$

Thanks to equations (33) and (37), we get:

$$\Delta\mu_i(\omega) = (\zeta_{ijk} \cdot E^j) * (D_v \cdot E^k)(\omega), \tag{40}$$

with:

$$\zeta_{ijk}(\omega) = g_k\ \partial\alpha_{ih}(\omega)\ \kappa^h{}_l\ \xi^l{}_j(\omega). \tag{41}$$

Equation (40) becomes:

$$\Delta\mu_i(\omega) = \int_{\mathbb{R}} \mathrm{d}\omega'\ \zeta_{ijk}(\omega - \omega')\ D_v(\omega')\ E^j(\omega - \omega')\ E^k(\omega'). \tag{42}$$

In our case, the incident electric field oscillates at the two frequencies ω_{vis} and ω_{IR}:

$$\begin{aligned} \mathbf{E}(\omega) &= \pi\Big(\delta(\omega - \omega_{\mathrm{vis}}) + \delta(\omega + \omega_{\mathrm{vis}})\Big)\mathbf{E}_{\mathrm{vis}} \\ &+ \pi\Big(\delta(\omega - \omega_{\mathrm{IR}}) + \delta(\omega + \omega_{\mathrm{IR}})\Big)\mathbf{E}_{\mathrm{IR}}. \end{aligned} \tag{43}$$

The constant vectors $\mathbf{E}_{\mathrm{vis}}$ and $\mathbf{E}_{\mathrm{IR}}$ depict the respective amplitudes of the visible and infrared input beams. Given the four delta functions of equation (43), the integral of equation (42) then gives four contributions corresponding to $\omega' = \pm\omega_{\mathrm{vis}}, \pm\omega_{\mathrm{IR}}$. Since we are interested in the vibrational response of the ligands, the terms which contain $D_v(\pm\omega_{\mathrm{vis}})$ are not relevant: the function D_v is only resonant in the IR range. Hence:

$$\begin{aligned} \Delta\mu_i(\omega) &= \zeta_{ijk}(\omega - \omega_{\mathrm{IR}})\ D_v(\omega_{\mathrm{IR}})\ E^j(\omega - \omega_{\mathrm{IR}})\ \pi E^k_{\mathrm{IR}} \\ &+ \zeta_{ijk}(\omega + \omega_{\mathrm{IR}})\ D_v(-\omega_{\mathrm{IR}})\ E^j(\omega + \omega_{\mathrm{IR}})\ \pi E^k_{\mathrm{IR}}. \end{aligned} \tag{44}$$

In time domain, since $\Delta\mu_i(t) = \frac{1}{2\pi}\int_{\mathbb{R}} \mathrm{d}\omega\ \Delta\mu_i(\omega)\ e^{-\imath\omega t}$, this translates into:

$$\begin{aligned} \Delta\mu_i(t) &= \frac{E^k_{\mathrm{IR}}}{2}\ \zeta_{ijk}(\omega_{\mathrm{vis}})\ D_v(\omega_{\mathrm{IR}})\ \pi E^j_{\mathrm{vis}}\ e^{-\imath\omega_{\mathrm{SFG}}t} \\ &+ \frac{E^k_{\mathrm{IR}}}{2}\ \zeta_{ijk}(-\omega_{\mathrm{vis}})\ D_v(-\omega_{\mathrm{IR}})\ \pi E^j_{\mathrm{vis}}\ e^{+\imath\omega_{\mathrm{SFG}}t} \\ &\quad [\text{for } \omega = \omega_{\mathrm{vis}} + \omega_{\mathrm{IR}} \mathrel{\hat{=}} \omega_{\mathrm{SFG}}] \\ &+ [\textit{idem} \text{ for } \omega = \omega_{\mathrm{vis}} - \omega_{\mathrm{IR}} \mathrel{\hat{=}} \omega_{\mathrm{DFG}}] \\ &+ [\textit{idem} \text{ for } \omega = 2\omega_{\mathrm{IR}} \mathrel{\hat{=}} \omega_{\mathrm{SHG}}] \\ &+ [\textit{idem} \text{ for } \omega = 0]. \end{aligned} \tag{45}$$

As expected, we retrieve the four nonlinear second-order processes: optical rectification ($\omega = 0$), second harmonic generation ($\omega = \omega_{\mathrm{SHG}}$), difference-frequency generation ($\omega = \omega_{\mathrm{DFG}}$) and sum-frequency generation ($\omega = \omega_{\mathrm{SFG}}$). Let us focus on this latter:

$$\Delta\mu_i(t) = \pi E^j_{\mathrm{vis}} E^k_{\mathrm{IR}}\ \mathrm{Re}\Big(\zeta_{ijk}(\omega_{\mathrm{vis}})\ D_v(\omega_{\mathrm{IR}})\ e^{-\imath\omega_{\mathrm{SFG}}t}\Big). \tag{46}$$

As $D'_v(\omega_v) = 0$ and since we are interested in the behaviour of the system around the resonance $\omega_{\rm IR} = \omega_v$, the relevant contribution to the SFG response is:

$$\begin{aligned}\Delta\mu_i(t) &= \pi E^j_{\rm vis} E^k_{\rm IR}\ D''_v(\omega_{\rm IR})\ \Big(\zeta'_{ijk}(\omega_{\rm vis})\sin(\omega_{\rm SFG}t) \\ &\quad -\zeta''_{ijk}(\omega_{\rm vis})\cos(\omega_{\rm SFG}t)\Big),\end{aligned} \tag{47}$$

where, for all complex function F, F' and F'' depict respectively its real and imaginary parts. Hence:

$$I_{\rm SFG} \propto \langle \Delta\mu_i^2(t)\rangle \propto |E^j_{\rm vis}|^2\ |E^k_{\rm IR}|^2\ \frac{|\zeta_{ijk}(\omega_{\rm vis})|^2}{(\omega_v-\omega_{\rm IR})^2+(\Gamma_v/2)^2}. \tag{48}$$

Thereby, we can identify the second-order susceptibility of the organic ligands:

$$\chi^{\rm org}_{ijk}(\omega_{\rm vis},\omega_{\rm IR}) \propto \frac{\zeta_{ijk}(\omega_{\rm vis})}{\omega_v-\omega_{\rm IR}+\imath\gamma_v}, \tag{49}$$

with $\gamma_v = \Gamma_v/2$. Given the definition of the tensor $\boldsymbol{\zeta}$, equation (41), $\chi^{\rm org}_{ijk}(\omega_{\rm vis},\omega_{\rm IR})$ is proportional to:

$$\underbrace{\partial\alpha_i{}^h(\omega_{\rm vis})}_{\substack{\text{Raman coupling of}\\ \text{the molecules under}\\ \text{visible excitation}}} \times\ \kappa_h{}^l\ \underbrace{\chi^{\rm QD}_{lj}(\omega_{\rm vis})}_{\substack{\text{electronic}\\ \text{response of NCs}\\ \text{in the visible}}} \times \underbrace{\frac{g_k}{\omega_v-\omega_{\rm IR}+\imath\gamma_v}}_{\substack{\text{IR absorption}\\ \text{of the molecules}}}. \tag{50}$$

We remind that tensor $\boldsymbol{\kappa}$ takes into account the fact that the local electric field produced by the exciton is not rigorously collinear with its dipole moment. For all that, due to the cristal structure of the QD, this non-collinearity does not play an important role. Especially, it does not condition the $\omega_{\rm vis}$-dependence of $\chi^{\rm org}_{ijk}(\omega_{\rm vis},\omega_{\rm IR})$. We can reasonably assume that $\boldsymbol{\kappa}$ is isotropic, that is proportional to the identity tensor: $\boldsymbol{\kappa} = \kappa\mathbf{1}$. Eventually, ignoring and skipping the constant factor of proportionality, we obtain:

$$\chi^{\rm org}_{ijk}(\omega_{\rm vis},\omega_{\rm IR}) \ =\ g_k\frac{\big[\partial\boldsymbol{\alpha}(\omega_{\rm vis})\ \boldsymbol{\chi}^{\rm QD}(\omega_{\rm vis})\big]_{ij}}{\omega_v-\omega_{\rm IR}+\imath\gamma_v}. \tag{51}$$

To conclude, each vibration mode v characterized by the eigenfrequency ω_v and the damping constant γ_v gives an SFG response driven by equation (51), as announced and discussed in the article.

Supplementary Note 4 – Molecular IR response. We have just detailed the method for deriving the molecular SFG nonlinear response within the formalism of normal modes. To legitimate this approach, we here apply our method to account for the molecular IR linear response.

We expand the transition dipole moment according to the normal coordinate Q:

$$\Delta\mu_i(\omega) = \underbrace{\left(\frac{\partial(\mu_0)_i}{\partial Q}\right)_0}_{=\ M_i} * Q(\omega). \tag{52}$$

Given equation (33):

$$\Delta\mu_i(\omega) = g_k\ M_i * (D_v\cdot E^k)(\omega) = \int_{\mathbb{R}} {\rm d}\omega'\ g_k\ M_i(\omega-\omega')\ D_v(\omega')\ E^k(\omega'). \tag{53}$$

For a monochromatic field $\mathbf{E}(t) = \mathbf{E}_{\rm IR}\cos(\omega_{\rm IR}t)$:

$$\mathbf{E}(\omega) = \pi\mathbf{E}_{\rm IR}\Big(\delta(\omega-\omega_{\rm IR})+\delta(\omega+\omega_{\rm IR})\Big), \tag{54}$$

what gives:

$$\Delta\mu_i(\omega) = \pi g_k E^k_{\rm IR}\Big(M_i(\omega-\omega_{\rm IR})\ D_v(\omega_{\rm IR}) + M_i(\omega+\omega_{\rm IR})\ D_v(-\omega_{\rm IR})\Big), \tag{55}$$

that is:

$$\Delta\mu_i(t) = \pi g_k E^k_{\rm IR} M_i(t)\underbrace{\Big(e^{-\imath\omega_{\rm IR}t}\ D_v(\omega_{\rm IR}) + e^{+\imath\omega_{\rm IR}t}\ D_v(-\omega_{\rm IR})\Big)}_{=2\cos(\omega_{\rm IR}t)D'_v(\omega_{\rm IR})+2\sin(\omega_{\rm IR}t)D''_v(\omega_{\rm IR})}. \tag{56}$$

At the resonance $\omega_{\rm IR} = \omega_v$, the real part of $D_v(\omega_{\rm IR})$ cancels. Thus, we approximate $\Delta\mu_i(t)$ by:

$$\Delta\mu_i(t) = 2\pi g_k E^k_{\rm IR} M_i(t)\sin(\omega_{\rm IR}t)D''_v(\omega_{\rm IR}). \tag{57}$$

Henceforth, the IR response is driven by:

$$\langle(\Delta\mu_i)^2\rangle \propto |E^k_{\rm IR}|^2\left(\frac{\partial\mu_i}{\partial Q}\right)^2_0\frac{g_k(\Gamma_v/2)^2}{(\omega_v-\omega_{\rm IR})^2+(\Gamma_v/2)^2}. \tag{58}$$

We formally retrieve the result obtained through quantum considerations, as reported in ref. [17], what definitely legitimates our calculation.

Supplementary References

[1] Haug, H. & Koch, S. *Quantum Theory of the Optical and Electronic Properties of Semiconductors* (World Scientific, 2009), fifth edn.

[2] Brus, L. E. Electron-electron and electron-hole interactions in small semiconductor crystallites: The size dependence of the lowest excited electronic states. *J. Chem. Phys.* **80**, 4403–4409 (1984).

[3] de Mello Donegá, C. & Koole, R. Size Dependence of the Spontaneous Emission Rate and Absorption Cross Section of CdSe and CdTe Quantum Dots. *J. Phys. Chem. C* **113**, 6511–6520 (2009).

[4] Richard, T., Lefebvre, P., Mathieu, H. & Allègre, J. Effects of finite spin-orbit splitting on optical properties of spherical semiconductor quantum dots. *Phys. Rev. B* **53**, 7287–7298 (1996).

[5] Noblet, T., Dreesen, L., Hottechamps, J. & Humbert, C. A global method for handling fluorescence spectra at high concentration derived from the competition between emission and absorption of colloidal CdTe quantum dots. *Phys. Chem. Chem. Phys.* **19**, 26559–26565 (2017).

[6] Efros, A. L. & Rosen, M. Quantum size level structure of narrow-gap semiconductor nanocrystals: Effect of band coupling. *Phys. Rev. B* **58**, 7120–7135 (1998).

[7] Kayanuma, Y. Wannier exciton in microcrystals. *Solid State Com.* **59**, 405–408 (1986).

[8] Malitson, I. H. A redetermination of some optical properties of calcium fluoride. *Appl. Opt.* **2**, 1103 (1963).

[9] Zhuang, X., Miranda, P. B., Kim, D. & Shen, Y. R. Mapping molecular orientation and conformation interfaces by surface nonlinear optics. *Phys. Rev. B* **59**, 12632–12640 (1999).

[10] Sapra, S. & Sarma, D. D. Evolution of the electronic structure with size in II-VI semiconductor nanocrystals. *Phys. Rev. B* **69**, 125304–125310 (2004).

[11] Yu, W. W., Qu, L., Guo, W. & Peng, X. Experimental Determination of the Extinction Coefficient of CdTe, CdSe, and CdS Nanocrystals. *Chem. Mater.* **15**, 2854–2860 (2003).

[12] Dagtepe, P., Chikan, V., Jasinski, J. & Leppert, V. J. Quantized Growth of CdTe Quantum Dots; Observation of Magic-Sized CdTe Quantum Dots. *J. Phys. Chem. C* **111**, 14977–14983 (2007).

[13] Groeneveld, E., Delerue, C., Allan, G., Niquet, Y.-M. & de Mello Donegá, C. Size Dependence of the Exciton Transitions in Colloidal CdTe Quantum Dots. *J. Phys. Chem. C* **116**, 23160–23167 (2012).

[14] Swafford, L. A. *et al.* Homogeneously Alloyed CdS_xSe_{1-x} Nanocrystals: Synthesis, Characterization, and Composition/Size-Dependent Band Gap. *J. Am. Chem. Soc.* **128**, 12299–12306 (2006).

[15] El-Qahtani, Z., Badawi, A., Easawi, K., Al-Hosiny, N. & Abdallah, S. Photoacoustic study of optical and thermal properties of alloyed $CdTe_xS_{1-x}$ nanocrystals. *Mater. Sci. Semicond. Process.* **20**, 68–73 (2014).

[16] Wilson, E. B., Decius, J. C. & Cross, P. C. *Molecular vibrations: The Theory of Infrared and Raman Vibrational Spectra* (Dover Publications, 1955).

[17] Hung, K.-K., Stege, U. & Hore, D. K. IR Absorption, Raman Scattering, and IR-Vis Sum-Frequency Generation Spectroscopy as Quantitative Probes of Surface Structure. *Appl. Spec. Rev.* **50**, 351–376 (2015).